Photomechanical investigations on post endodontically rehabilitated teeth

A. Kishen
A. Asundi
Nanyang Technological University
School of Mechanical and Production Engineering
Actuators and Sensors Strategic Research Program
Singapore 639798, Singapore

Abstract. An investigation of the stress distribution patterns in post–core restored teeth and the behavior of dentin material to fracture propagation was conducted using experimental techniques such as digital photoelasticity (on photoelastic models), mechanical testing and scanning electron microscopy (SEM) (on extracted teeth). Digital photoelastic experiments showed that endodontic post–core restoration resulted in regions of high tensile stress and of stress concentrations in the remaining dentin structure. It was observed from mechanical testing that the fracture resistance in post–core restored teeth is significantly lower ($p < 0.0001$) than that in intact tooth. There was a significant correspondence between the plane of stress concentrations identified in the photoelastic models and in those of the plane of fracture exhibited by the rehabilitated tooth specimens. While the fracture of post–core rehabilitated teeth was consistent, that of control teeth was not as distinct. The SEM highlighted varying dentin response to fracture propagation at the inner core and the outer regions. The fractographs showed brittle and ductile response to fracture propagation in the outer and inner core dentin, respectively. These photomechanical studies highlighted that the stress concentrations, high tensile stress and loss of inner ductile dentin associated with post endodontic rehabilitation diminished their resistance to fracture. © *2002 Society of Photo-Optical Instrumentation Engineers.* [DOI: 10.1117/1.1463046]

Keywords: fractographs; phase shift; photoelasticity; post core; post endodontic; stress.

Paper JBO-001011 received Jan. 31, 2001; revised manuscript received Nov. 2, 2001; accepted for publication Nov. 15, 2001.

1 Introduction

The structure of the tooth which remains after endodontic treatment is usually undermined by previous episodes of caries, fracture, and tooth preparation. However practitioners regularly utilize a stiff post–core system to restore the mutilated tooth after endodontic treatment. Although these restorations are supposed to compensate for changes inflicted in the tooth by pathology and treatment procedures, tooth fractures, breakage of the restoration, secondary caries, and root perforations are common causes of failure in a post endodontically restored tooth.[1]

It is established that many detrimental effects produced during rehabilitative procedures are due to a lack of understanding of biomechanical principles underlying the treatment.[2] Biomechanical studies are crucial to highlight the behavior of a post endodontically restored tooth to functional forces. Previous studies of endodontic posts primarily focused on the retention and design aspects of the endodontic post.[3–5] They also investigated continuous and intermittent load resistance on clinically sound endodontically treated teeth.[6,7] In these studies it was concluded that preservation of the tooth's structure would provide maximum resistance to tooth fracture.

Contrary to the above conclusion recent concepts in root canal preparations have emphasized thorough cleaning and shaping of the root canals to obtain three-dimensional obturation of the root canal systems and thereby achieve long-term success with endodontic therapy. The foremost purpose of this study is to examine the relationship between the nature of stress distribution and the patterns of fracture in a post–core restored lower anterior incisor tooth. A digital photoelastic evaluation is used for the former, while mechanical testing and subsequent fractographic analysis using scanning electron microscopy are employed for the latter. Mandibular central incisors are considered for the present analysis since they possess minimal bulk and minimal mesial–distal width. These analyses could help in anticipating the demands placed on artificial biomaterials and devices when they are used to rehabilitate a tooth with minimal bulk.

An advanced digital phase shift photoelastic experiment is utilized to study the biomechanical effects of the endodontic post and core in the dentin structure. Although photoelasticity is an established experimental technique applied to dental biomechanics, conventional photoelasticity exhibits certain shortcomings.[2,8–10] The digital phase shift photoelastic technique developed by the authors for dental applications not only allows experimentation of anatomical size models but also permits quantitative interpretation of the images with high sensitivity and accuracy.[11] Furthermore, the phase shift method used for processing digitized fringes has the important

Address all correspondence to Dr. Anil Kishen. Tel: (65) 790-6324; Fax: (65) 7912274; E-mail: ekishen@ntu.edu.sg

advantage of being capable of identifying the sign of fringe orders. This advantage facilitates identification of compressive and tensile stress regions. All the above features make this technique appropriate for analyzing complex stress patterns.

2 Materials and Methods

The experiments consisted of two parts. In the first part, digital photoelastic stress analysis was conducted on post–core restored teeth models. In the second part, experiments were conducted on extracted teeth specimens using a mechanical tester. These experiments were conducted to determine the load to fracture in extracted teeth specimens and in teeth rehabilitated using the post core. Further, the fractured teeth specimens were subjected to detailed SEM examination. The SEM due to its high resolution and depth of field could reveal topographical features of the fractured dentin. The fractographs provided insight into the response of dentin material to the propagation of cracks.

2.1 Part I: Digital Photoelastic Analysis

Photoelasticity is based on the stress-optic effect, which for plane stress analysis is governed by the following stress-optic law:[12]

$$\sigma_1 - \sigma_2 = \frac{\theta}{2\pi} \frac{f_\sigma}{h} = \frac{N f_\sigma}{h}, \qquad (1)$$

where $(\sigma_1 - \sigma_2)$ is the difference in the in-plane principal stress, $\theta/2\pi$ is the resultant optical phase generated due to stress birefringence in the model, f_σ is the material fringe value and h is the thickness of the specimen. Since the values of f_σ and h are constant, the most important aspect for analysis of stress distribution is recording the optical phase (θ) or fringe orders $(N = \theta/2\pi)$ at every point of interest on the fringe pattern.[11]

2.1.1 Model Preparation

Two types of sectional models were fabricated for the digital photoelastic experiments:

- model (I) simulated an intact (normal) lower central incisor tooth and the supporting bone;
- model (II) simulated a lower central incisor tooth rehabilitated using post and core restoration and the supporting bone (Figure 1).

Model fabrication was done using a digitized outline of human mandible obtained from a cadaver. The coordinates obtained from the digitized image were fed into a computer numerical control (CNC) machine to fabricate the models from photoelastic sheets (PSM-1, measurement groups). A layer of chemically cured silicone rubber 0.35 mm thick was used to simulate the periodontal ligament and a specially manufactured polyester reinforced composite sheet 0.15 mm thick was used to simulate root cementum.[11] This sheet was chosen because it had an elastic modulus similar to that of the model but with higher resilience. A dental composite (Charisma from Kulzer) was used to prepare the enamel portion of the model.[11]
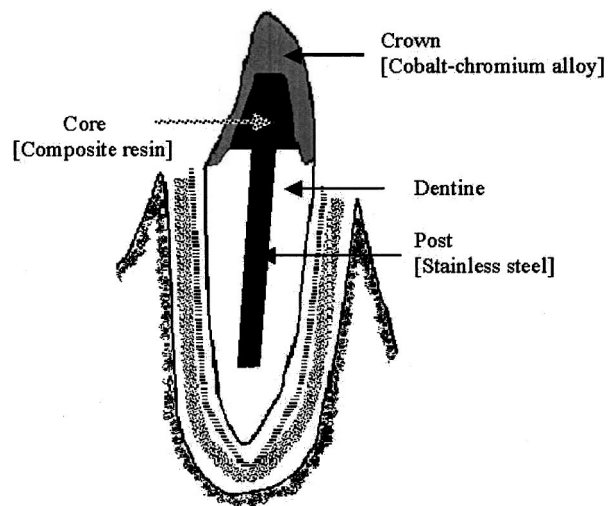

Fig. 1 Model of a rehabilitated tooth and supporting bone.

The models simulating a rehabilitated tooth were prepared with two thirds of the incisal crown removed. A parallel-sided stainless steel post, 0.9 mm in diameter was utilized as the post and core restoration was prepared using dental composite material (BIS-CORE, BISCO Inc., U.S.). The crown was fabricated using a cobalt–chromium casting alloy (Vitallium). Glass ionomer luting cement (Fuji I) was used for luting the post and crown into position. Five models of intact normal teeth (model I) and post and core rehabilitated teeth (model II) were prepared for testing.

2.1.2 Experiments

The experimental setup consisted of a circular polariscope and an image processing system (Figure 2). A special loading device was fabricated that applied loads along the long axis (0°) and 60° lingual to the long axis of the tooth. A load cell fixed on the upper portion of the loading device measured the load applied. During the experiments the loading device with the model was placed in the circular polariscope. Four phase-
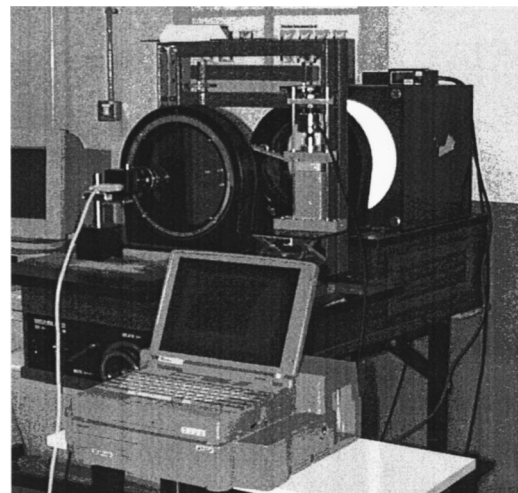

Fig. 2 Experimental arrangement consisting of a conventional circular polariscope and an image processing system.

stepped images were obtained at each load by rotating the analyzer at 0°, 45°, 90°, and 135° angles with respect to the polarizer. The fringe patterns obtained were acquired using a high resolution charge coupled device (CCD) camera [753(H)×244(V) pixels] and stored in a digital computer. The four images were then evaluated using a traditional phase stepping algorithm to obtain a wrapped phase map.[11,13] Phase unwrapping was done on select lines to make the fringe modulation continuous and to obtain information on the nature of the stress distribution. The system was calibrated (f_σ) and then confirmed for accuracy by testing a calibrated disk.[11] All models were tested three times at different loads ranging from 25 to 150 N along the direction of the long axis of the tooth (0°) and at 60° lingual to the long axis of the tooth. All five models in each group were tested to confirm the repeatability of the experiments.

2.2 Part II: Fractographic Analysis

2.2.1 Specimen Preparation

Twenty freshly extracted human mandibular incisor teeth of similar dimensions [approximately 20 mm in length (8.5 mm crown length and 11.5 mm root length)] were selected and maintained in phosphate buffered saline medium (0.1 M phosphate buffer, pH of 7.2) for the study. These specimens were randomly divided into two equal groups.

- Group (1): Teeth rehabilitated using post–core and full-crown restorations.
- Group (2): Intact teeth, used as the control.

The tooth specimens in group (1) were initially decoronated 3 mm coronal to the cemento-enamel junction (CEJ). This was done to simulate teeth that were to receive post–core restoration. Each tooth in group (1) was prepared from size No. 20 to a size No. 45 file, 1 mm short of the root's apex. During instrumentation, normal saline solution was used to irrigate the root canals and medium size absorbent points were used to dry the root canals.

The post space in the teeth specimens [group (1)] was prepared 4 mm short of the root's apex by a twist drill (Whaledent, U.S.). A stainless steel smooth sided parallel post (Para-post, Whaledent) 0.9 mm in diameter and 10 mm in length was cemented using glass ionomer cement (Fuji I). Core restoration for a height of 3 mm was prepared using composite resin (BIS-CORE, BISCO, Inc.). Once the core restoration was complete, full-crown preparation was done with a chamfer preparation 2 mm apical to the core. The full crown was induction cast in a cobalt–chromium casting alloy (Vitallium), air dried, and cemented using the same glass ionomer cement. Excess cement was removed after the crown was completely set and the tooth specimens were placed in physiological saline for 24 h before testing.

The surface of the root of the teeth was applied with 0.5 mm thick soft green wax, the thickness of which is approximately equal to the average thickness of the periodontal ligament. The teeth were stabilized within a silicone mold so that the long axis of the root would be 60° toward the direction of the load applied during the fracture test. A cold cure acrylic resin was introduced into the mold and the teeth were gently removed when the first signs of polymerization occurred. The
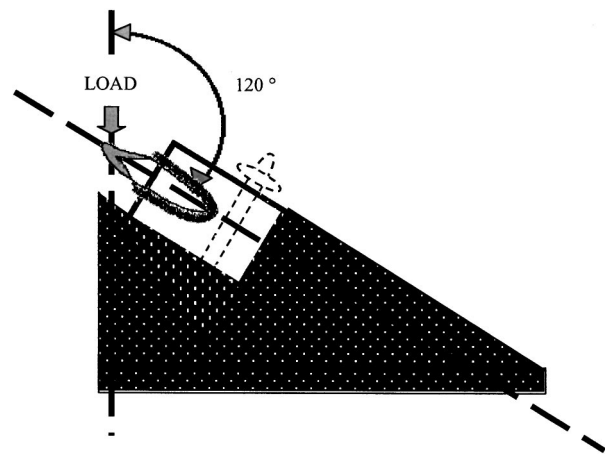
Fig. 3 Schematic diagram indicating the angles of loading in the Instron material tester.

wax spacer was later removed from the surface of the root and a self-curing silicone rubber was injected into the acrylic block to simulate periodontal ligament. The root was mounted in the acrylic resin block with approximately two thirds of the root within the block and one third extending outward.

2.2.2 Experiment (1): Mechanical Test

The test specimen along with the acrylic resin mold was placed in an Instron testing machine (Figure 3) using a special device that allowed the tooth to be loaded at an angle 120° towards its long axis. This particular angle was chosen to reproduce typical transverse loading.[14] Transverse forces have been identified as the most destructive forces at the crown's post–root interface and earlier investigators utilized similar angles for fracture resistance analysis.[7,15] During testing, failure load, which is defined as the maximum load that a specimen can withstand before catastrophic failure, occurred and the mode of failure was recorded for all specimens. Controlled loads were applied to the teeth at a crosshead speed of 2.5 mm/min.[15]

2.2.3 Experiment (2): Fractography

In the fractography analysis the fractured teeth specimens were mounted to directly examine the fracture plane using scanning electron microscopy. Since it was found that the fracture planes were relatively flat and microscopically featureless, the specimen mounted within the microscope's chamber was tilted from 12° to 50° for better visualization and interpretation of the fracture topography.

3 Results

3.1 Part I: Digital Photoelastic Analysis

3.1.1 Nature of Stress Distribution in Normal (Intact) Teeth

Figure 4 shows typical isochromatic fringe patterns in the intact tooth [model (I)] at 25, 80, and 125 N occlusal loads directed along the long axis of the tooth. It was found that the stress patterns indicated significant bending in the cervical region [Figure 5(A)] and the midregion of the root [Figure
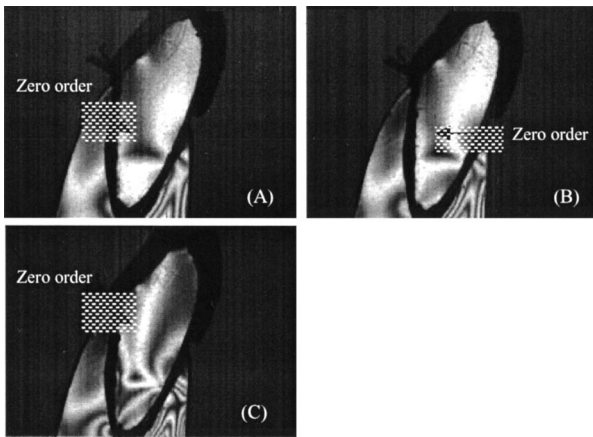
Fig. 4 Typical isochromatic fringe patterns in model I (intact tooth) for occlusal loads of (A) 25, (B) 80, and (C) 125 N directed along the long axis of the tooth.

5(B)], and substantially high compressive stress on the facial side in comparison to the tensile stress on the lingual side. There was a reduction in bending stress towards the apical region, with only compressive stress evident in this region
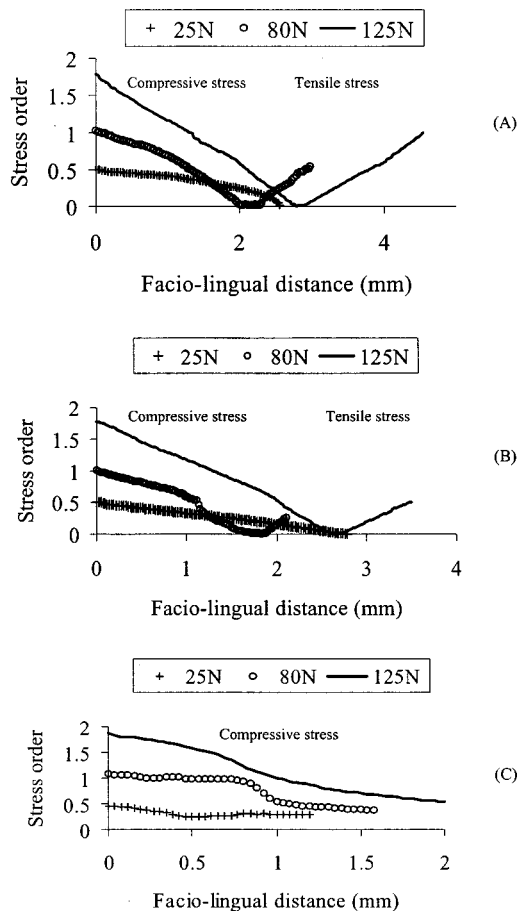

Fig. 5 Stress distribution patterns in the intact tooth (model I) at (A) the cervical third, (B) middle third, and (C) apical third of the root for different occlusal loads applied along the long axis of the tooth (1 stress order = 2.2 MPa stress).
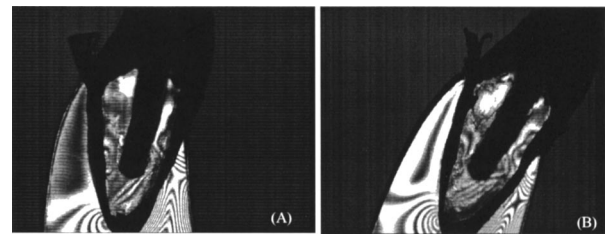

Fig. 6 Typical isochromatic fringe patterns in model II (rehabilitated tooth) for an occlusal load of 80 N directed (A) along the long axis and (B) 60° lingual to the long axis of the tooth.

[Figure 5(C)]. A zero order fringe was identified within the tooth (Figure 4). The compressive and tensile stress orders identified during bending were reconfirmed using a fingernail test.[11]

It was also found that when occlusal loads are increased from 25 to 125 N the bending stress increased in the cervical and middle regions, with the compressive stress conspicuously larger than the tensile stress. However, only compressive stress was observed along the apical region of the tooth. Although there was an increase in the magnitude of compressive stress there was no significant variation in the nature of the stress distribution when the angle of occlusal loads changed from 0° to 60°. Moreover, no significant concentration of stress was observed along the tooth specimen during the entire experiment.

3.1.2 Nature of Stress Distribution in Rehabilitated Teeth

Figure 6 shows typical isochromatic fringe patterns in a rehabilitated tooth [model (II)] loaded at 80 and 125 N, along the direction of the long axis of the tooth and Figure 7 shows a phase wrapped image of the rehabilitated tooth model (II),
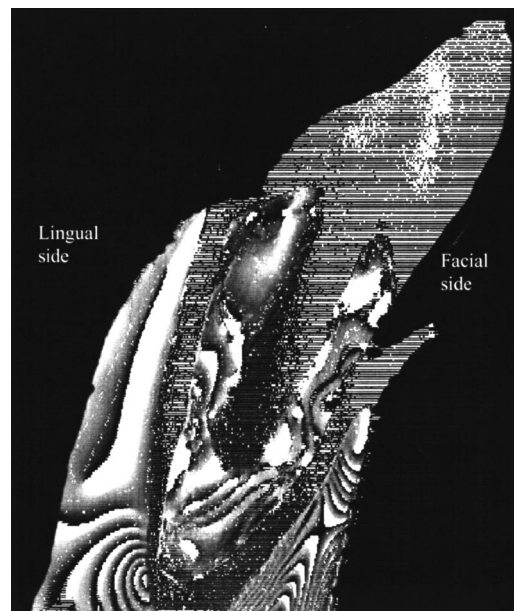

Fig. 7 Phase wrapped image obtained from the four-phase shifted images in a rehabilitated tooth (model II), loaded at 125 N, 60° lingual to the long axis of the tooth.
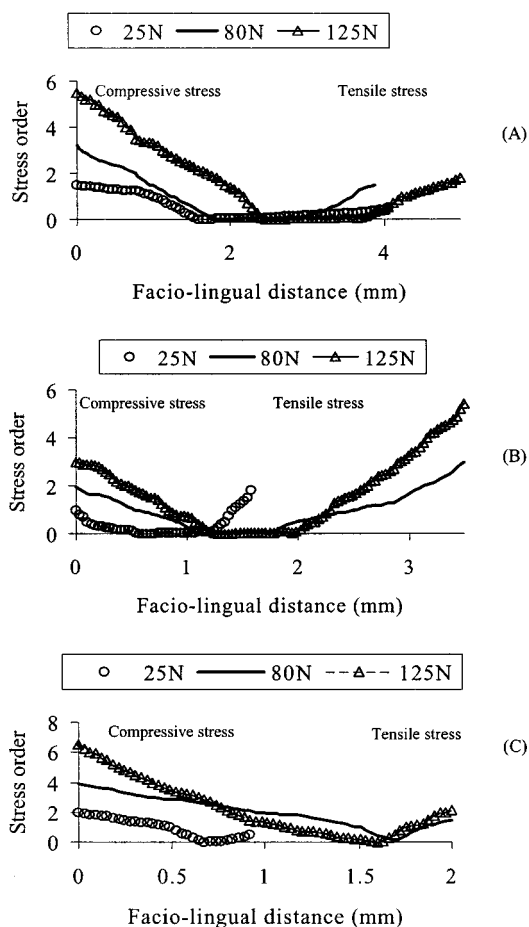
Fig. 8 Stress distribution patterns in a rehabilitated tooth (model II) at the (A) cervical, (B) middle, and (C) apical regions for different occlusal loads applied along the long axis of the tooth (1 stress order = 2.2 MPa stress).

loaded at 125 N at an angle of 60° in the direction of the long axis of the tooth. It was found that there was a significant increase in the magnitude of stress within the tooth. Increased bending stress was identified in the cervical region and in the middle region of the root. This resulted in higher compressive stress in the cervical region (facial side) and higher tensile stresses in the midregion (lingual side). There was a reduction in bending stress towards the apical region (Figure 8). At higher loads, concentrations of compressive stress on the facial side and of tensile stress on the lingual side of the tooth are observed. In addition, the lingual side of the apical region adjacent to the post also produced tensile stress.

3.2 Part II: Fractographic Analysis

3.2.1 *Experiment (1): Mechanical Test*

It was found that the average load required to fracture teeth specimens rehabilitated using the post and core system (group 1) was 23.303 kg (std. dev.: 5.859) and the average loads required to fracture control teeth (group 2) was 49.40 kg (std. dev.: 4.236) (Figure 9). The unpaired student t test showed a statistically significant difference ($p < 0.0001$) in the load required to fracture teeth specimens rehabilitated using the post and core (group 1) and control teeth (group 2). It was noticed that rehabilitated teeth specimens exhibited oblique fracture of the root, extending from the facial side (cervical region) to the lingual side (midregion) (Figure 10). However the modes of fractures in the intact teeth specimens (control) were not characteristic. Upon examination of the fractured specimens using SEM, several observations were made (see Sec. 3.2.2).

3.2.2 *Experiment (2): Fractography*

The results of fractography are now discussed. *Rehabilitated teeth specimens*. The following observations were made

- The fracture progressed from the core region (adjacent to the root canal) towards the outer surface. Thumbnail impressions indicating the initiation of cracks were observed adjacent to the root canal [Figures 11(A) and 11(B)].
- The outer dentin on the facial and the lingual sides exhibited predominantly smooth cleavage planes, which is characteristic of the brittle mode of fracture propagation [Figure 12(A)].
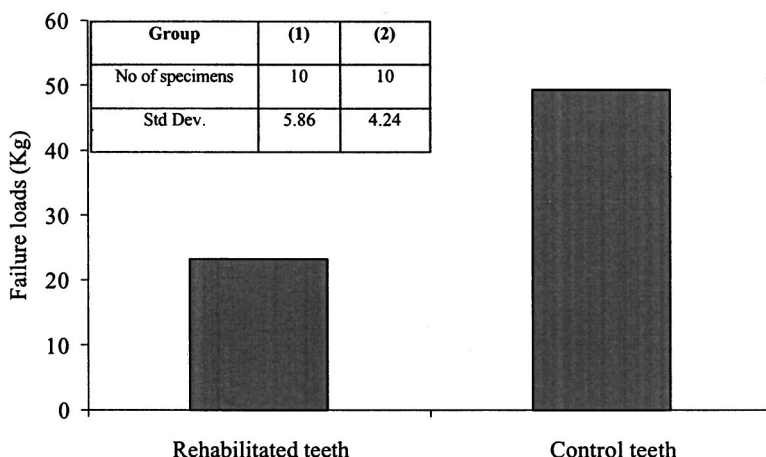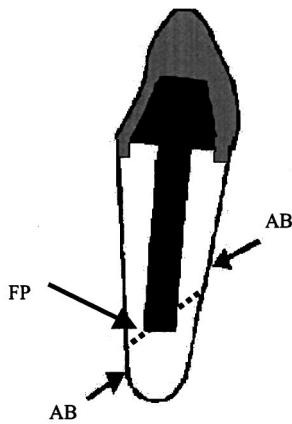

Fig. 9 Histogram that compares the resistance to failure in intact teeth and that of post–core rehabilitated teeth specimens.
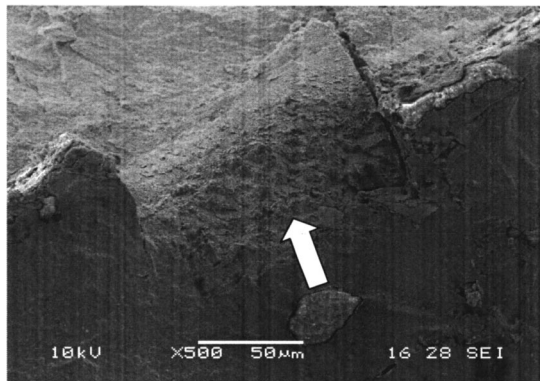
AB: Direction of reactant forces from the supporting alveolar bone
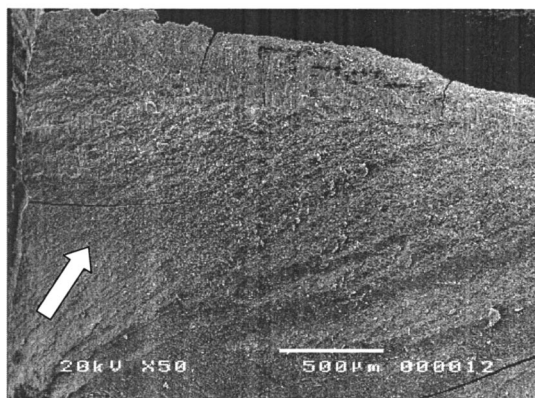FP: Fracture plane in rehabilitated tooth

Fig. 10 Schematic diagram showing the plane of fracture in a rehabilitated tooth specimen.

- The inner dentin (near the root canal) showed a more corrugated fracture pattern, suggesting quasibrittle behavior [Figure 12(B)].

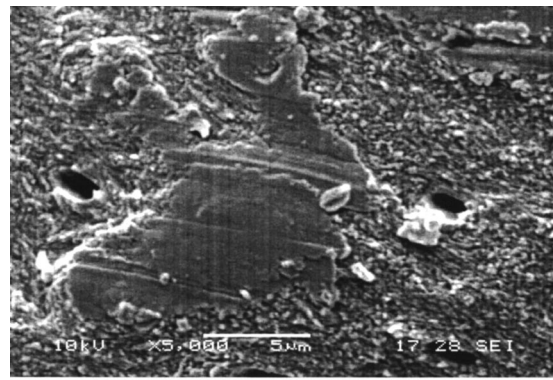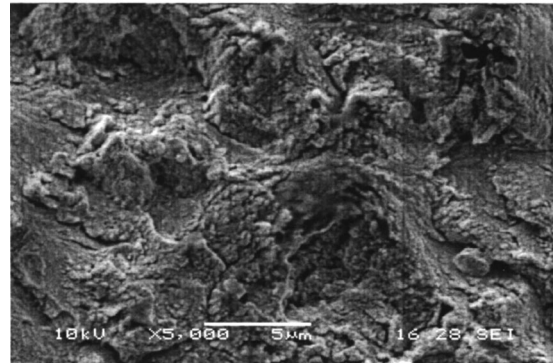*Control teeth specimens*. We observed the following.

Fig. 11 SEM image showing (A), (B) thumbnail impressions of the origin of fracture adjacent to the root canal.

Fig. 12 SEM image showing (A) a smooth dentinal cleavage plane (brittle) in the outer part and (B) a corrugated dentinal surface (quasibrittle) in the inner part of the dentin of a fractured rehabilitated tooth specimen.

- The outer dentin displayed some cracks, while the inner dentin showed evidence of corrugations on the surface of the fracture [Figure 13(A)].
- The inner core dentin material (adjacent to the root canal) revealed fibrous elongations in the vicinity of advancing cracks [Figure 13(B)]. These features, found in the inner dentin of the control teeth, are more indicative of ductile material behavior.

4 Discussion

Stress is produced within a structure as a result of load acting upon it. The direction of the load applied and the shape of the structure influence the nature of the distribution of stress within the structure. Also, any imperfections such as notches or cracks within the structure cause a localized increase in the magnitude of the stress, referred to as the stress concentration. Concentrations of stress from a biomechanical perspective indicate regions of potential failure due to the formation of cracks or fatigue.

The digital photoelastic experiments showed that the tooth structures exhibited characteristic patterns that suggested bending along the cervical region and the midregion of the root dentin. Bending stress consists of compressive stress on one side (concave) and tensile stress on the other side (convex) of the neutral axis or zero stress zone. In these experiments although bending displayed compressive and tensile stress on the cervical and midregions of the root, the maximum compressive stress is larger than the maximum tensile
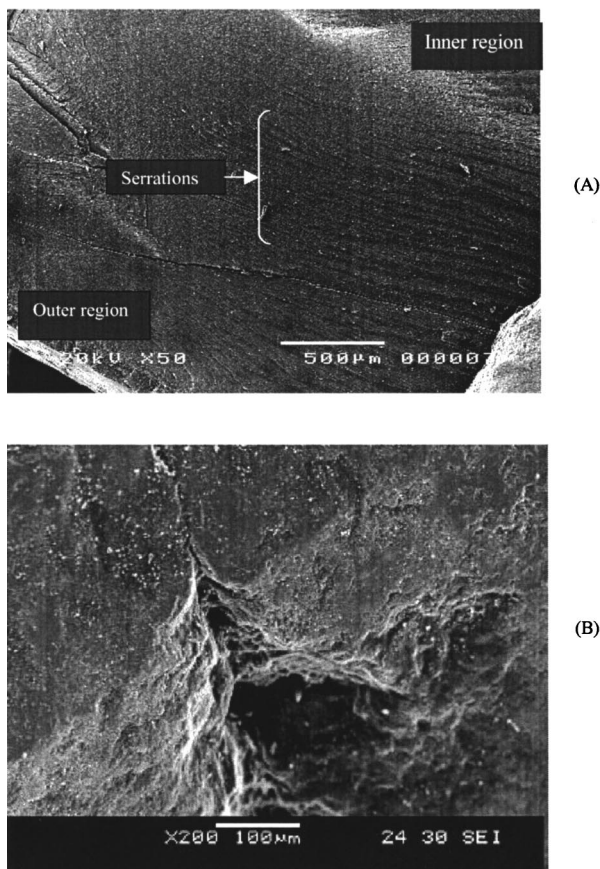
Fig. 13 SEM image showing (A) serrations in the inner dentinal surface and (B) dentin material elongation at the advancing tip of the crack in a control tooth specimen.

stress. However, there is a significant reduction in bending towards the root's apex with only compressive stress conspicuous in the apical region. This unique nature of stress distribution associated with the intact tooth is mainly attributed to the geometry of the tooth and its supporting structure.[11] In the intact tooth (model I) the root canal is not simulated. This primarily facilitated identification of stress in relation to normal dental pulp, which is found to be zero.

In the case of the rehabilitated tooth (model II) the post and core restoration and cementing of the post and crown are done using routine restorative materials. Although this photoelastic modeling is time consuming, it helped in achieving a more realistic experimental model for analysis. The pattern of stress distribution in the rehabilitated tooth, contrary to in the normal tooth, displayed conspicuously high tensile stress and regions of stress concentrated in the remaining tooth structure (Figures 5 and 8). It is important to note that earlier studies have confirmed that the tensile strength of dentin is considerably lower than its compressive strength.[16] Therefore the increased tensile stress associated with post–core restoration in a rehabilitated tooth could be deleterious to the remaining dentin structure.

The stress concentrations identified in the rehabilitated teeth are attributed to the location of the endodontic post, higher stiffness of the post and core restorative material and the directions of the occlusal load. The development of stress concentration in the region adjacent to the apex of the endodontic post is in agreement with previous finite element analysis.[17,18] The stress concentration identified in the cervical region of the tooth was in congruence with the three-dimensional finite element analysis conducted by Ho et al.[19]
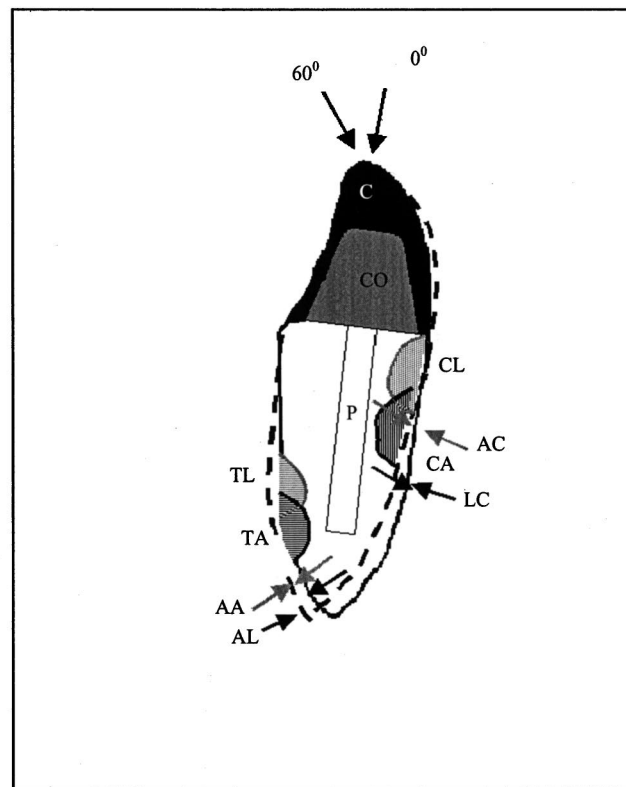
In this investigation fractographic analyses are conducted to determine the resistance of post–core restored teeth to fracture and to examine how the dentin material responds to fracture propagation. Although dynamic or cyclical tests may closely model the manner in which dental restorations fail, the present static test also validates the relative resistance to stress of various restorative devices.[20] The fractographic analysis is carried out to obtain *in vitro* data of extracted teeth specimens that are comparable with the results obtained from the experimental models in digital photoelasticity. Therefore a static mode of a fracture test that closely approximates stress analysis is preferred.

Engineering theory states that the strain in the material adjacent to a hole in a structure will be two or more times higher than the stress if the hole were not present.[21] The increase in strain in the materials or in tissues around such a ''defect'' means that even a minimal stress concentration can initiate failure in these regions. It is crucial to understand that in a rehabilitated tooth much dentin material is removed from the core (adjacent to the root canal) during cleaning and shaping procedures of the root canal and post preparation. Consequently a root canal space, which is thin ribbon or oval shaped in cross section, is altered into a large round configuration. This causes a drop in fracture resistance in post and core restored teeth results.

The ratio of the failure load of the altered structure to the failure load of the intact structure is said to be one measure of the reduction in structural strength. Hence it could be rationalized from our analysis that there is a reduction in dentin strength of 47.17% due to dentin removal and restorative treatment procedures. This finding is consistent with previous studies, which suggest that dentin removal diminished fracture resistance, and that rehabilitative restorations did not improve the strength of treated teeth.[15,22] Moreover, the load to fracture exhibited by the rehabilitated teeth and control teeth in this study displayed close agreement with the results obtained in previous experiments by Gluskin et al.[23]

It is of interest to observe that the plane of fracture in rehabilitated teeth corresponded with the plane of stress concentrations identified in the digital photoelastic experiments. Besides, previous studies done to compare the resistance to intermittent loading of teeth with cast post cores and with prefabricated parallel sided posts–composite cores showed all teeth specimens to exhibit oblique root fractures.[24] The plane of the root fracture observed in the Isidor and Brondum study agreed with the plane of fracture observed in this study.

The fractographs revealed that the radicular fractures in the post–core rehabilitated teeth specimens initiated from the core dentin (adjacent to the root canal) and progressed towards the outer surface. Similar findings were reported in previous *in vitro* studies of experiments on cast post and partial core design.[25] Further, the fractographs obtained from scanning electron microscopy displayed a different response of the dentin surface to fracture propagation. Dentin in the outer part of the tooth exhibited a smooth cleavage plane, which is characteristic of brittle fractures, while dentin in the

C-Crown   CO-Core   P-Post
CL-Compressive stress concentration for loads along the long axis of the tooth (cervical region)
CA- Compressive stress concentration for loads at 60^0 lingual to the long axis (cervical region)
AC- Supporting bone contact for loads at 60^0 lingual to the long axis of the tooth (cervical region)
LC- Supporting bone contact for loads along the long axis of the tooth (cervical region)
TL- Tensile stress concentration for loads along the long axis of the tooth (apical region)
TA- Tensile stress concentration for loads at 60^0 lingual to the long axis of the tooth (apical region)
AA- Supporting bone contact for loads at 60^0 lingual to the long axis of the tooth (apical region)
AL- Supporting bone contact for loads along the long axis of the tooth (apical region)

Fig. 14 Schematic diagram illustrating the stress concentration regions in a tooth rehabilitated using endodontic post core crown for occlusal loads that act along the long axis of the tooth and 60° lingual to the long axis.

inner part of the tooth (in proximity to the root canal) exhibited a corrugated and tearing pattern; this could be termed quasibrittle or ductile behavior.

It is significant to note that the nature of the mineralization in dentin identified in our earlier analysis corresponded with the present behavior of dentin material to fracture propagation.[26] The outer dentin (peritubular dentin) that is highly mineralized exhibited a brittle mode of fracture propagation, whereas the inner dentin (mantle dentin), which is less mineralized exhibited the ductile mode of fracture propagation. Subsequently, the brittle dentin in the outer part would offer less resistance to fracture propagation compared to the inner dentin. It is essential to note that earlier studies of bones have demonstrated an association between a high degree of mineralization and low values of work of fracture (which is a measure of fracture toughness) and vice versa. The low fracture toughness associated with the high degree of mineralization was caused by the inhibition of various crack-stopping mechanisms with a high volume fraction of minerals.[27]

It is important to realize that a tooth loses core dentin material due to both the disease process and the treatment procedure. Subsequently, when the tooth is restored using post–core restoration, it is observed that the *post–core tooth* system bends like an integral unit along with the remaining dentin structure during function and thereby alters the nature of the stress distribution within the existing tooth structure. Consequently, high tensile stress and stress concentrations are produced in the remaining dentin structure (Figure 14). Further, the fractographic analysis has shown that the highly mineralized outer dentin exhibits a conspicuously brittle mode of fracture propagation that should offer less resistance to fractures. This will cause the post–core restored tooth to become weak. It is suggested that, in order to obtain post–core restoration that substitutes tooth strength to its ''near'' original state, it is important to engineer endodontic post–core restoration that does not induce stress concentrations and high tensile stress for the remaining dentin structure. Further, replacement of the lost inner, fracture resistant, ductile dentin with a suitable restorative material should also be considered.

5 Conclusions

Photomechanical experiments were carried out to evaluate the stress distribution pattern in post endodontically rehabilitated

teeth and to examine the behavior of dentin material to fracture. These investigations highlighted the behavior of a post–core rehabilitated tooth to functional forces. The following conclusions were drawn from these experiments.

1. The endodontic post resulted in substantially high tensile stress and regions of stress concentrations in the remaining dentin structure.

2. The fracture resistance of the rehabilitated teeth was conspicuously lower than that of intact normal teeth.

3. The plane of stress concentration identified in the *in vitro* models of rehabilitated teeth (digital photoelasticity) coincided with the plane of fracture exhibited by the rehabilitated extracted teeth subjected to mechanical testing.

4. The fractographs of the outer dentin exhibited a brittle response to fracture propagation, while those of the inner core dentin displayed ductile response to fracture propagation.

References

1. F. S. Weine, *Endodontic Therapy*, 5th ed., pp. 756–801, Mosby, St. Louis (1996).
2. A. A. Caputo and J. P. Standlee, *Biomechanics in Clinical Dentistry*, pp. 19–28, Quintessence, Chicago (1987).
3. A. G. Mentink, N. H. Creugers, P. M. Hoppenbrouwers, and R. Meeuwissen, "Qualitative assessment of stress distribution during insertion of endodontic posts in photoelastic material," *J. Dent.* **26**, 125–131 (1998).
4. B. I. Cohen, S. Condos, B. L. Musikant, and A. S. Deutsch, "Pilot study comparing the photoelastic stress distribution for four endodontic post systems," *J. Oral Rehabil.* **23**, 679–685 (1996).
5. G. D. Mattison, "Photoelastic stress analysis of cast-gold endodontic posts," *J. Prosthet. Dent.* **48**, 407–411 (1982).
6. K. C. Trabert, A. A. Caputo, and M. Abou-Rass, "Tooth fracture—A comparison of endodontic and restorative treatments," *J. Endod.* **4**, 341–345 (1978).
7. G. E. Guzy and J. I. Nicholls, "*In vitro* comparison of intact endodontically treated teeth with and without endo-post reinforcement," *J. Prosthet. Dent.* **42**, 39–41 (1979).
8. Mahler and Peyton, "Photoelasticity as a research technique for analysing stresses in dental structures," *J. Dent. Res.* **34**, 831–838 (1955).
9. J. P. Standlee, A. A. Caputo, E. W. Collard, and M. H. Pollack, "Analysis of stress distribution by endodontic posts," *Oral Surg., Oral Med., Oral Pathol.* **33**, 952–960 (1972).
10. J. P. Standlee, A. A. Caputo, and J. P. Holcomb, "The Dentatus screw: Comparative stress analysis with other endodontic dowel designs," *J. Oral Rehabil.* **9**, 23–33 (1982).
11. A. Asundi, and A. Kishen "Digital photoelastic investigations on the tooth-bone interface," *J. Biomed. Opt.* **6**, 224–230 (2001).
12. J. W. Dally and W. F. Riley, *Experimental Stress Analysis*, 3rd ed., pp. 425–429, McGraw–Hill, New York (1991).
13. A. Asundi, "Phase shifting in photoelasticity," *Exp. Tech.* **17**, 19–23 (1993).
14. H. G. Kurer, "The classification of single-rooted, pulpless teeth," *Quintessence Int.* **22**, 939–943 (1991).
15. J. A. Sorensen and M. J. Engelman, "Ferrule design and fracture resistance of endodontically treated teeth," *J. Prosthet. Dent.* **63**, 529–536 (1990).
16. M. L. Lehman, "Tensile strength of human dentin," *J. Dent. Res.* **46**, 197–201 (1967).
17. K. R. Williams and J. T. Edmundson, "A finite element stress analysis of an endodontically restored tooth," *Eng. Med.* **13**, 167–173 (1984).
18. J. G. Cailleteau, M. R. Rieger, and J. E. Akin, "A comparison of intracanal stresses in a post-restored tooth utilizing the finite element method," *J. Endod.* **18**, 540–544 (1992).
19. M. H. Ho, S. Y. Lee, H. H. Chen, and M. C. Lee, "Three-dimensional finite element analysis of the effects of posts on stress distribution in dentin," *J. Prosthet. Dent.* **72**, 367–372 (1994).
20. R. W. Loney, M. B. Moulding, and R. G. Ritsco, "The effect of load angulations on fracture resistance of teeth restored with cast post and cores and crowns," *J. Prosthodont.* **8**, 247–251 (1995).
21. F. Pauwels, *Biomechanics of the Locomotor Apparatus*, p. 506, Springer, Berlin (1980).
22. M. Trope, D. O. Maltz, and L. Tronstad, "Resistance to fracture of restored endodontically treated teeth," *Endod. Dent. Traumatol.* **1**, 108–111 (1985).
23. A. H. Gluskin, R. A. Radke, S. L. Frost, and L. G. Watanabe, "The mandibular incisor: Rethinking guidelines for post and core design," *J. Endod.* **21**, 33–37 (1995).
24. F. Isidor and K. Brondum, "Intermittent loading of teeth with tapered, individually cast or prefabricated, parallel-sided posts," *Int. J. Prosthodont.* **5**, 257–261 (1992).
25. A. Patel and D. L. Gutteridge, "An *in vitro* investigation of cast post and partial core design," *J. Dent.* **24**, 281–287 (1996).
26. A. Kishen, U. Ramamurty, and A. Asundi, "Experimental studies on the nature of property gradients in human tooth," *J. Biomed. Mater. Res.* **51**, 650–659 (2000).
27. J. D. Currey, "Effects of differences in mineralisation on the mechanical properties of bone," *Philos. Trans. R. Soc. London Bone Biol. Sci.* **13**, 509–518 (1984).